Revisiting the global budget of atmospheric glyoxal: updates on terrestrial and marine precursor emissions, chemistry, and impacts on atmospheric oxidation capacity

Aoxing Zhang[1,2], Tzung-May Fu[1,2,3], Yuhang Wang[4], Enyu Xiong[1,2,5], Wenlu Wu[1,2,6], Yumin Li[7], Lei Zhu[1,2], Wei Tao[1,2], Kelley C. Wells[8], Dylan B. Millet[8], Zhe Wang[9], Bin Yuan[10], Min Shao[10], Christophe Lerot[11,12], Thomas Danckaert[11], Ruixiong Zhang[13], and Kelvin H. Bates[14]

[1]State Key Laboratory of Soil Pollution Control and Safety, Shenzhen Key Laboratory of Precision Measurement and Early Warning Technology for Urban Environmental Health Risks, School of Environmental Science and Engineering, Southern University of Science and Technology, Shenzhen, Guangdong 518055, China
[2]Guangdong Provincial Field Observation and Research Station for Coastal Atmosphere and Climate of the Greater Bay Area, Southern University of Science and Technology, Shenzhen, Guangdong 518055, China
[3]National Center for Applied Mathematics Shenzhen, Shenzhen, Guangdong 518055, China
[4]School of Earth and Atmospheric Sciences, Georgia Institute of Technology, Atlanta, GA, 30342, USA
[5]Department of Civil and Environmental Engineering, The Hong Kong Polytechnic University, SAR, Hong Kong, 999077, China
[6]Institute for Climate and Atmospheric Science, School of Earth and Environment, University of Leeds, Leeds LS2 9JT, U.K.
[7]Institute for Atmospheric and Climate Science, ETH Zurich, Zurich 8092, Switzerland
[8]Department of Soil, Water, and Climate, University of Minnesota, St Paul, MN 55108, USA
[9]Division of Environment and Sustainability, The Hong Kong University of Science and Technology, Hong Kong SAR, China
[10]Institute for Environmental and Climate Research, Jinan University, Guangzhou, Guangdong 511443, China
[11]Royal Belgian Institute for Space Aeronomy (BIRA-IASB), Brussels 1180, Belgium
[12]now at constellr S.A., Liège 4031, Belgium
[13]Atlassian US Inc., San Francisco, CA 94104, USA
[14]Department of Mechanical Engineering, University of Colorado Boulder, Boulder, CO 80309, USA

Correspondence: Tzung-May Fu (fuzm@sustech.edu.cn) and Yuhang Wang (yuhang.wang@eas.gatech.edu)

Note S1. Calculation of glyoxal yields using DSMACC

Our DSMACC simulations were set to the meteorological and chemical environments of a surface location in Southern China (Zou et al., 2023). The meteorological and chemical variables were fixed based on measurements from a field campaign in Hong Kong SAR, China (Xiong et al., 2025) : atmospheric surface pressure 1007 hPa; surface temperature 293 K; 5×10^3 ppm of H_2O (relative humidity of 22%), 0.7 ppm of CO, 40 ppb of O_3.

To constrain the production and concentration of OH in the model, two proxy compounds (named OHPRE and OHDECAY) were added in the mechanisms as a producer and consumer of OH. Under a typical NO_X concentration (1 ppb), we constrained a baseline OHPRE and OHDECAY to get a daily mean OH production rate of 1.3×10^6 molecules cm^{-3} s^{-1} with daily mean OH concentration of 1.6×10^6 molecules cm^{-3}. We conducted sensitivity simulations with NO concentrations ranging from 0.1 ppb to 5 ppb, assuming an ambient NO_2 to NO concentrations ratio of 4. At each NO_X sensitivity experiment, we preturb OHPRE and OHDECAY by scale factors from 0.01 to 100, in order to cover real conditions of NO_X and OH concentrations in the atmosphere.

To quantify the glyoxal yields from different mechanisms, we constructed three distinct DSMACC models: D-MCM, D-GC, and D-GCnew. The D-MCM model incorporated the photochemical degradation of isoprene from MCM v3.3.1, which includes 611 intermediate species and 1944 chemical reactions, representing the most comprehensive representation of isoprene chemistry currently available. The D-GC and D-GCnew models adopted the default isoprene chemical mechanisms from GEOS-Chem version 14.2.3 and the updated mechanisms developed in this study, respectively. DSMACC used the Kinetic Pre-Processor (KPP) (Sandu and Sander, 2006; Lin et al., 2023) to process kinetics chemical mechanisms. KPP used implicit solver to deal with fast chemical reactions with radicals, making the chemical state in DSMACC sensitive to the radical production rate. Because not all radicals sources was included in DSMACC experiments, the radical production rates were different from the real condition and were more sensitive to NO_X concentrations. Therefore, rather than constraining HO_X concentrations, we created a dummy OH source in DSMACC to produce OH radicals as a constant rate (1.3×10^6 molec cm^{-3} s^{-1})

To quantify glyoxal yields from isoprene, we initialized the model with 1 ppb isoprene for all experiments. we turned off the chemical reactions removing glyoxal in all DSMACC experiments, and the simulation periods are 96 hours, much larger than the lifetime of isoprene. Then the ratio of the final glyoxal concentration and the precursor's initial concentration is the glyoxal yield derived from DSMACC.

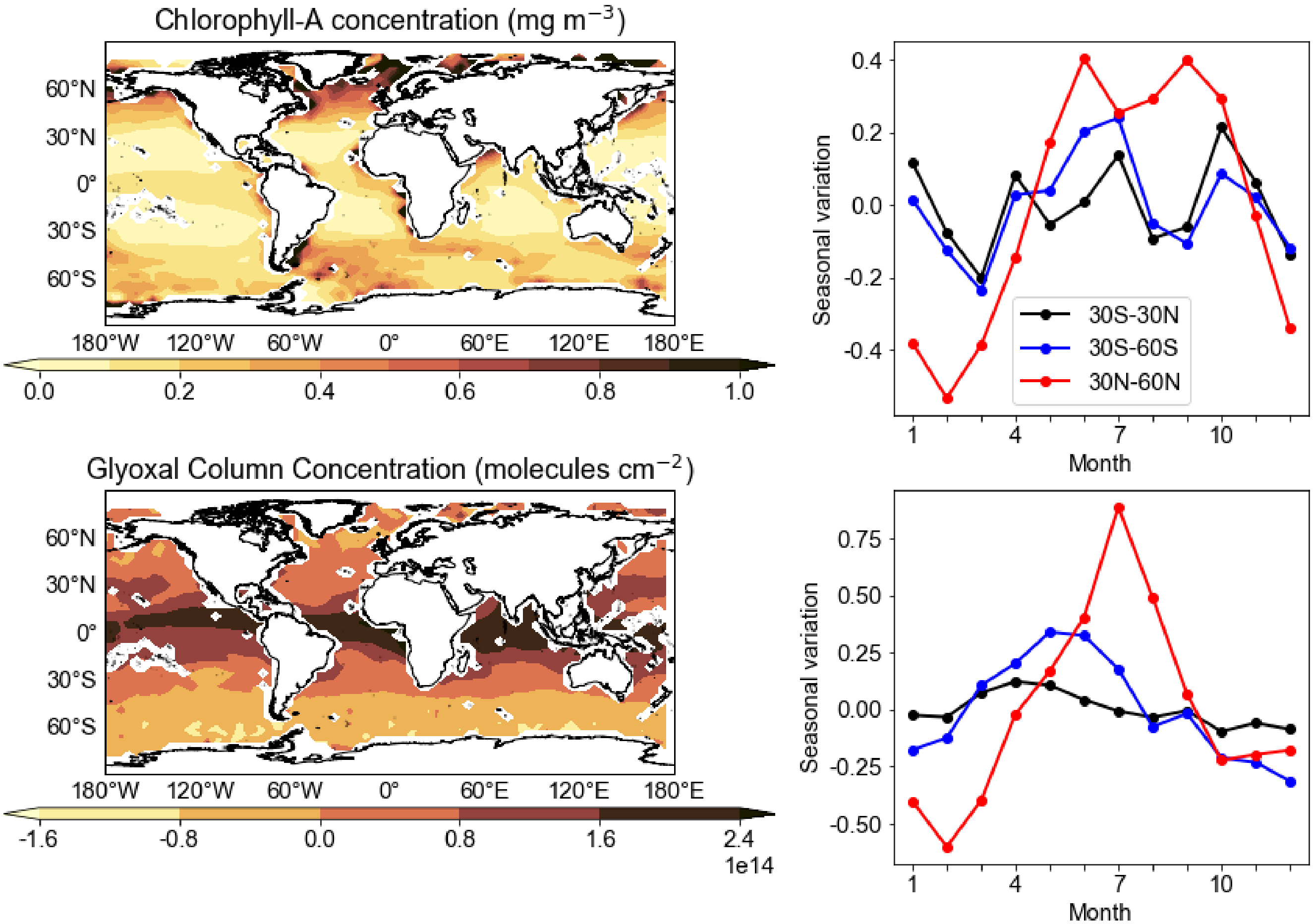

Figure S1. The annual mean and seasonal variation of MODIS surface Chlorophyll-A concentrations and TROPOMI glyoxal column concentrations over the ocean. The season variation represents the variation of each monthly mean relative to the annual mean.

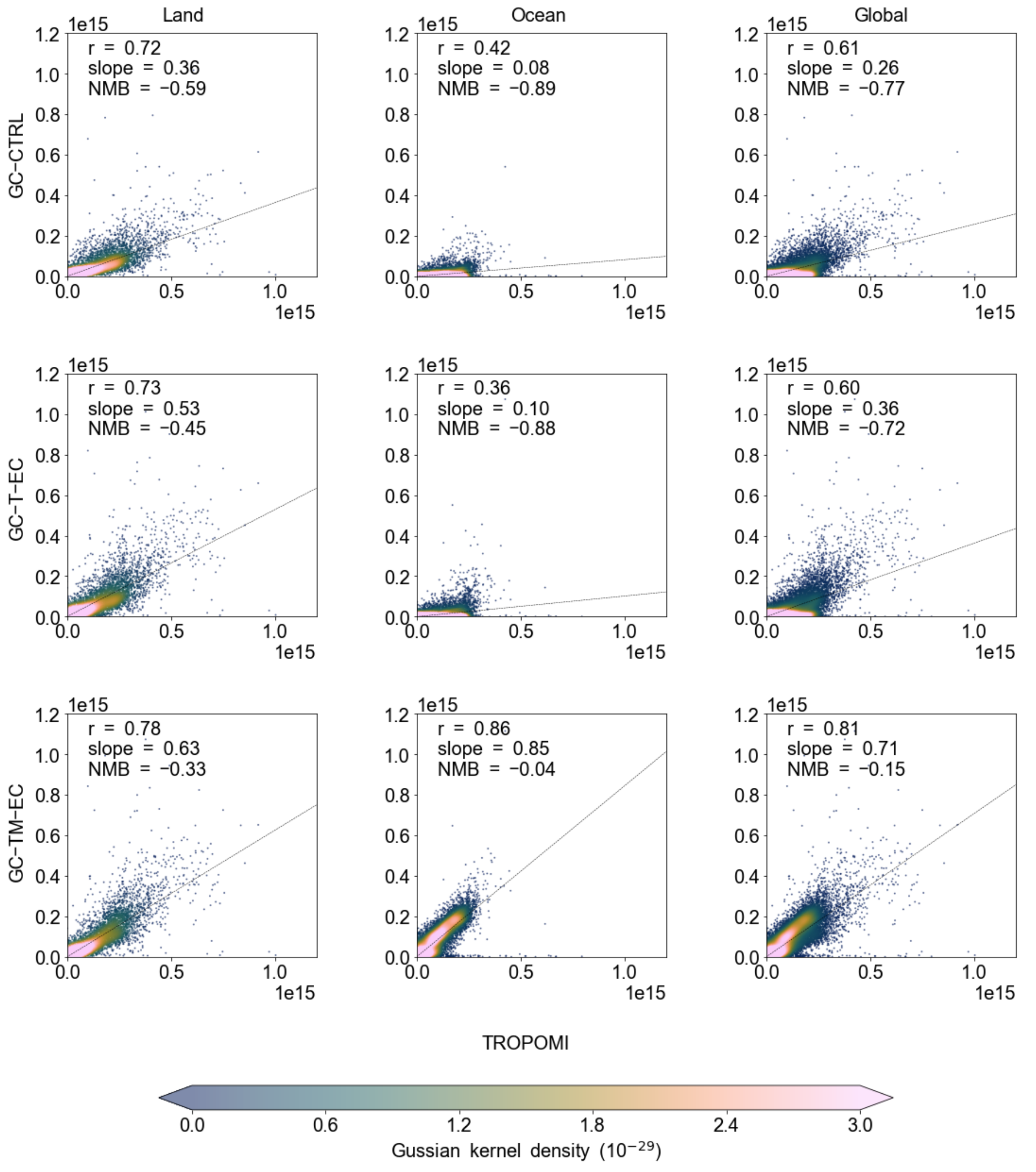

Figure S2. Glyoxal column concentration (molecules cm^{-2}) of TROPOMI observation and GEOS-Chem simulations (GC-CTRL and GC-TM-EC) over land and ocean. Each scatter represents a monthly mean glyoxal column concentration over a $4^{\circ} \times 5^{\circ}$ grid box.

Table S1. Observed Glyoxal Concentration.

Name	Latitude	Longitude	Period	Hour of Day	Glyoxal (ppt)
Ocean					
Salt Point[1]	39°N	123°W	Aug Sep 2005	11-14 Local time	20
Carribean Sea[2]	15°N	66°W	Oct 1988	Daily mean	40
Sargasso Sea coast[3]	15°N - 27°N	94°W - 66°W	Oct 1988 Mar 1989	Daily mean	80
Tropical Pacific NH[4]	5°N - 20°N	133°W - 110°W	Jan Mar 2012	Daily mean	32
Tropical Pacific SH[4]	5°S - 10°S	110°W - 93°W	Jan Mar 2012	Daily mean	43
TP NH aircraft RF12[5]	8.5°N	101.5°W	Jan Feb 2012	Daily mean	25
TP NH aircraft RF17[5]	6°N - 7°N	90°W - 92°W	Jan Feb 2012	Daily mean	34
Cape Grim[6]	40°S - 44°S	140°E - 144°E	Aug Sep 2011	Daily mean	7
Chatham Rise[6]	40°S - 50°S	175°E - 175°W	Feb Mar 2012	Daily mean	23
Tropical Eastern Pacific Ocean[7]	15°S - 5°N	85°W - 95°W	Nov 2008 Jan 2009	Daily mean	67
Cape Verde[8]	17°N	25°W	Jun Sep, 2014	Daily mean	5.6
WISE[9]	40°N - 70°N	10°W - 10°E	Sep Oct 2017	Daily mean	19
CAFE[9]	6°S - 35°N	40°W - 3°E	Aug 2018	Daily mean	44
EMeRGe-ASIA[9]	17°N - 33°N	122°E - 135°E	Mar 2018	Daily mean	75
SouthTRAC[9]	43°S - 60°S	34°W - 75°W	Oct 2019	Daily mean	10
Land					
ACRIDICON–CHUVA [10]	12°S - 2°N	51°W - 68°W	Sep 2014	Daily mean	87
Hong Kong [11]	22.217°N	114.25°E	Nov 2020- Feb 2021	10-15 Local time	45
Xingtai [12]	37.18°N	114.37°E	Aug 2021	6-18 LT	80
YMK [13]	22.55°N	114.60°E	Sep-Oct 2019	Daily mean	289
Guangzhou [14]	23°N	113.2°E	Sep-Nov 2018	Daily mean	1
HGS[15]	22.728°N	112.929°E	Jan 2017	Daily mean	100
Mt. Hua[16]	34.48°N	110.08°E	Aug 2020	Daily mean	330
Tazhong[17]	38.97°N	83.66°E	May-Jun 2018	Daily mean	210
Mt. Hua[18]	34.48°N	110.083°E	Aug 2020	Daily mean	260
Shanghai[19]	31.34°N	121.51°E	Jun-Aug 2018	Daily mean	162
Mt. Fuji-May[20]	32.81°N	130.73°E	May 2016	Daily mean	30
Mt. Fuji-Dec[20]	32.81°N	130.73°E	Dec 2016	Daily mean	5
BEARPEX[21]	38.88°N	120.62°W	Jul 2009	Daily mean	33

(Continued)

Table S1. Observed Glyoxal Concentration. (Continued)

MCMA-2003[22]	19.5°N	99°W	Apr 2003	Daily mean	270
Shanghai[23]	31.19°N	121.43°E	May-Jun 2021	Daily mean	0.6
Hefei-MAM[24]	31.78°N	117.2°E	Mar 2018-May 2018	8-17 Local time	230
Hefei-JJA[24]	31.78°N	117.2°E	Jun 2018-Aug 2018	8-17 Local time	220
Hefei-SON[24]	31.78°N	117.2°E	Sep 2018-Nov 2018	8-17 Local time	220
Hefei-DJF[24]	31.78°N	117.2°E	Dec 2018-Feb 2019	8-17 Local time	230
Elizabeth-MAM[25]	40.66°N	74.21°W	Mar-May 2000-2001	Daily mean	718
Elizabeth-JJA[25]	40.66°N	74.21°W	Jun-Aug 1999- 2000	Daily mean	706
Elizabeth-SON[25]	40.66°N	74.21°W	Sep-Nov, 1999-2000	Daily mean	509
Elizabeth-DJF[25]	40.66°N	74.21°W	Dec-Feb, 1999-2001	Daily mean	448
Lhasa[26]	29.63°N	91.02°E	Aug 2000	Daily mean	400
Madrid-MAM[27]	40.44°N	3.69°E	Mar 2016-May 2016	9 Local time	1410
Madrid-JJA[27]	40.44°N	3.69°E	Jun 2016-Aug 2016	9 Local time	1040
Madrid-SON[27]	40.44°N	3.69°E	Sep 2016-Nov 2016	9 Local time	980
Madrid-DJF[27]	40.44°N	3.69°E	Dec 2016, Jan-Feb 2016	9 Local time	1400
Chongqing[28]	29.83°N	107.01°E	Dec 2018-Jan 2019	9-16 Local time	80
Montelibretti[29]	42.11°N	12.63°E	Jul-Sep 2005	8-16 Local time	440
Palaiseau-summer[30]	48.71°N	2.21°E	Jul 2009	Daily mean	47
Palaiseau-winter[30]	48.71°N	2.21°E	Jan-Feb 2010	Daily mean	158
Rio de Janeiro-May[31]	22.86°N	43.26°W	May 1999	Daytime	201
Rio de Janeiro-JJA[31]	22.86°N	43.26°W	Jul-Aug 2000	Daytime	126
Rio de Janeiro-SON[31]	22.86°N	43.26°W	Sep-Nov 2000	Daytime	99
Blodgett Fores[32]	38.9°N	120.63°W	Aug-Sep 2000	8-21 Local time	27
Bukit Atur[33]	4.8°N	117.83°E	Apr-jul 2008	Daily mean	335
Mt. Tai[34]	36.25°N	117.1°E	Jun 2006	Daily mean	188
Tomakomai Forest[35]	42.73°N	141.52°E	Sep 2003	Daily mean	27
Melbourne-MAM[36]	37.69°S	144.95°E	Mar-May 2017-2019	6-17 Local time	164
Melbourne-JJA[36]	37.69°S	144.95°E	Jun-Aug, 2017-2018	6-17 Local time	139
Melbourne-SON[36]	37.69°S	144.95°E	Sep-Nov, 2017-2018	6-17 Local time	142
Melbourne-DJF[36]	37.69°S	144.95°E	Dec-Feb 2016-2019	6-17 Local time	134
Beijing[37]	39.9°N	116.41°E	Jun 2017	Daily mean	116
CalNex2010[38]	34°N	118°W	Jun 2017	Daily mean	103

(Continued)

Table S1. Observed Glyoxal Concentration. (Continued)

BEACHON-ROCS[39]	39°N	105°W	May-Jun 2010	Daily mean	28
Madison[40]	43°N	89°W	Aug 2010	Daily mean	38
Alabama[41]	33°N	87°W	May 2011	Daily mean	29
SOAS[42]	33°N	87°W	Jun-Jul 2013	Daily mean	33
Northern Michigan[43]	45.5°N	84.72°W	Jun-Jul 2013	Daily mean	30
Simcoe[44]	43°N	80°W	Jul 2008	Daily mean	500
Wuhan [45]	31°N	114°E	Aug 2021	Daily mean	420
Amazon-DJF [47]	2.1°S	59°W	Dec 2019 - Feb 2020	Daily mean	70
Amazon-MAM [47]	2.1°S	59°W	Mar-May 2020	Daily mean	55
Amazon-JJA [47]	2.1°S	59°W	Jun-Aug 2019	Daily mean	69

Amazon-SON [47]	2.1°S	59°W	Sep-Nov 2019	Daily mean	80

[1] Seaman et al. (2006)
[2] Zhou and Mopper (1990b)
[3] Zhou and Mopper (1990a)
[4] Coburn et al. (2014)
[5] Volkamer et al. (2015); 0-2 km mean
[6] Lawson et al. (2015)
[7] Sinreich et al. (2010)
[8] Walker et al. (2022)
[9] Kluge et al. (2023); 0-2 km mean
[10] Wendisch et al. (2016); 0-2 km mean
[11] Xu et al. (2023)
[12] Wang et al. (2019)
[13] Zhu et al. (2021)
[14] Wu et al. (2020)
[15] Chang et al. (2019)
[16] Zhang et al. (2024)
[17] Geng et al. (2022)
[18] Qi et al. (2023)
[19] Guo et al. (2021)
[20] Mitsuishi et al. (2018)
[21] DiGangi et al. (2012)
[22] Volkamer et al. (2007)
[23] Chen et al. (2025), below detection limit (0.0012 ppb)
[24] Hong et al. (2022)
[25] Liu et al. (2006)
[26] Li et al. (2022)
[27] Benavent et al. (2019)
[28] Xing et al. (2020)
[29] Possanzini et al. (2007)
[30] Ait-Helal et al. (2014)
[31] Grosjean et al. (2002)
[32] Spaulding et al. (2003)
[33] MacDonald et al. (2012)
[34] Kawamura et al. (2013)
[35] Ieda et al. (2006)
[36] Fayad et al. (2020)
[37] Liang et al. (2013)
[38] Washenfelder et al. (2011)
[39] Wolfe et al. (2014)
[40] Henry et al. (2012)
[41] Kaiser et al. (2016)
[42] Hettiyadura et al. (2017)
[43] Johnson (2008)
[44] Aiello and McLaren (2009)
[45] (Huang et al., 2023)
[46] Donner et al. (2024)

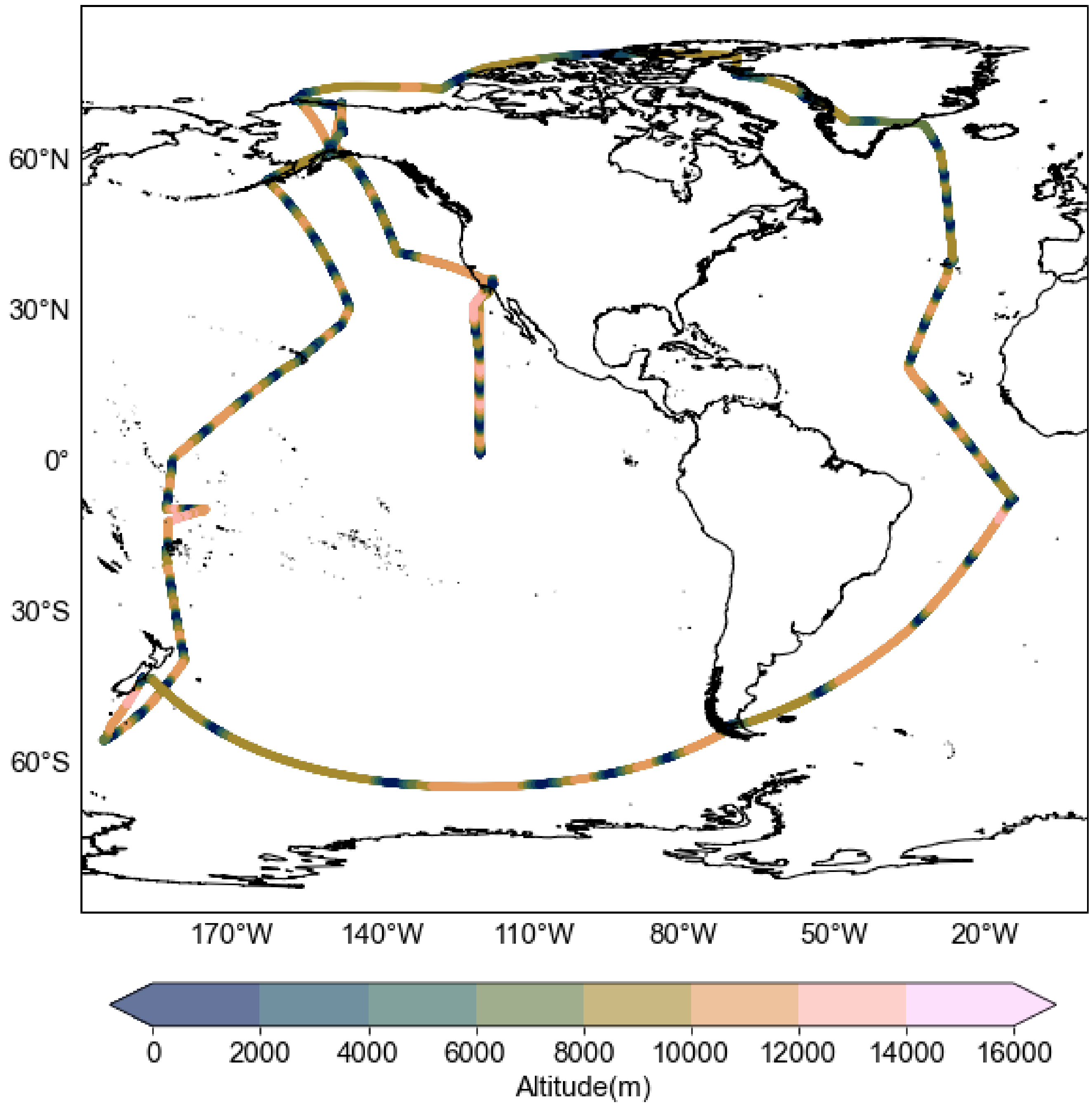

Figure S3. The flight track of the ATom-2 mission.

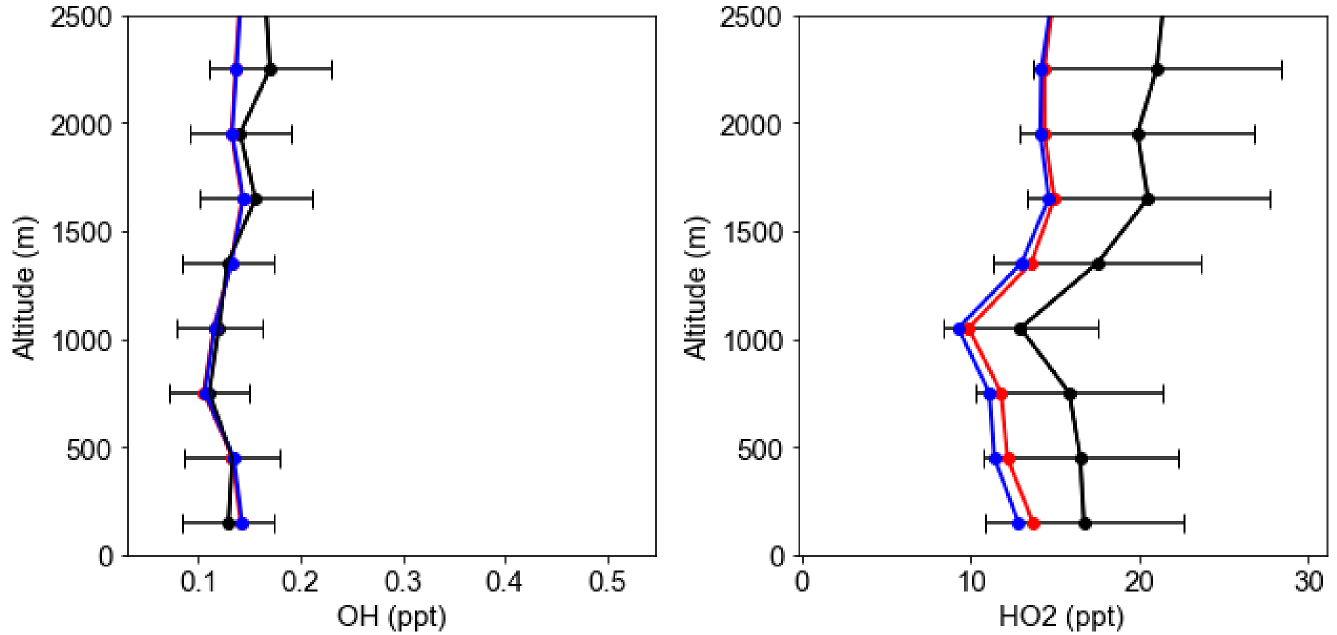

Figure S4. The vertical profiles of ATom-2 aircraft measurements over the tropical ocean (20°S-20°N) and corresponding simulated OH and HO_2 concentration (GC-CTRL in blue; GC-TM-EC in red) within the MBL.

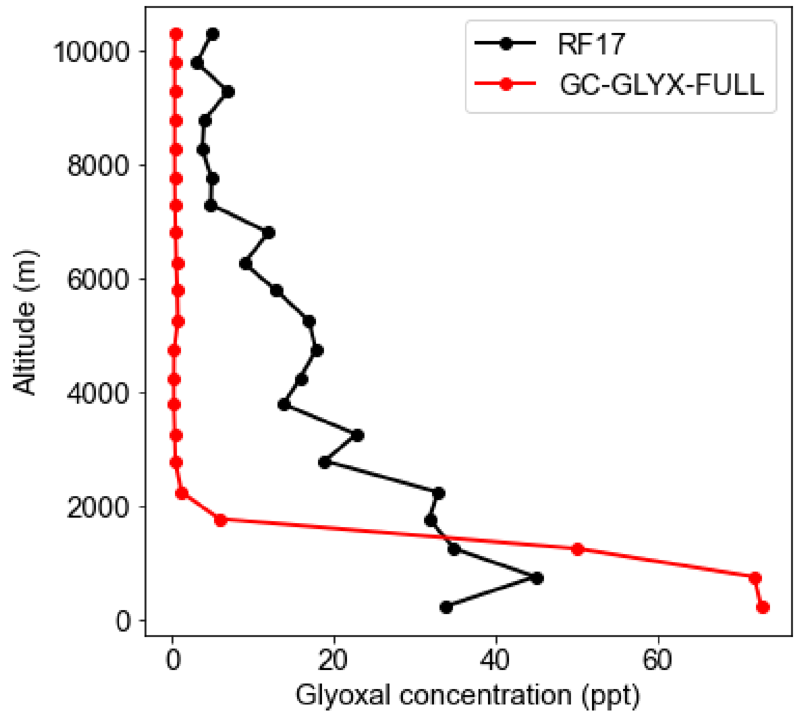

Figure S5. The vertical profile of glyoxal measured by Volkamer et al. (2015) during RF17, and the vertical profile in the corresponding location and month from the model simulation with marine glyoxal production included.

References

Aiello, M. and McLaren, R.: Measurement of Airborne Carbonyls Using an Automated Sampling and Analysis System, Environmental Science & Technology, 43, 8901–8907, https://doi.org/10.1021/es901892f, 2009.

Ait-Helal, W., Borbon, A., Sauvage, S., de Gouw, J. A., Colomb, A., Gros, V., Freutel, F., Crippa, M., Afif, C., Baltensperger, U., Beekmann, M., Doussin, J.-F., Durand-Jolibois, R., Fronval, I., Grand, N., Leonardis, T., Lopez, M., Michoud, V., Miet, K., Perrier, S., Prévôt, A. S. H., Schneider, J., Siour, G., Zapf, P., and Locoge, N.: Volatile and intermediate volatility organic compounds in suburban Paris: variability, origin and importance for SOA formation, Atmospheric Chemistry and Physics, 14, 10 439–10 464, https://doi.org/10.5194/acp-14-10439-2014, 2014.

Benavent, N., Garcia-Nieto, D., Wang, S., and Saiz-Lopez, A.: MAX-DOAS measurements and vertical profiles of glyoxal and formaldehyde in Madrid, Spain, Atmospheric Environment, 199, 357–367, https://doi.org/10.1016/j.atmosenv.2018.11.047, 2019.

Chang, D., Wang, Z., Guo, J., Li, T., Liang, Y., Kang, L., Xia, M., Wang, Y., Yu, C., Yun, H., Yue, D., and Wang, T.: Characterization of organic aerosols and their precursors in southern China during a severe haze episode in January 2017, Science of The Total Environment, 691, 101–111, https://doi.org/10.1016/j.scitotenv.2019.07.123, 2019.

Chen, Y., Xu, Y., Huang, D., Lai, D., Chen, Y., Guo, J., Feng, X., Hui, L., Wang, Q., Huang, C., Wang, H., and Wang, Z.: Photochemical impacts of atmospheric carbonyl compounds on ozone formation and radical chemistry in urban Shanghai, Environmental Pollution, 380, 126 557, https://doi.org/10.1016/j.envpol.2025.126557, 2025.

Coburn, S., Ortega, I., Thalman, R., Blomquist, B., Fairall, C. W., and Volkamer, R.: Measurements of diurnal variations and eddy covariance (EC) fluxes of glyoxal in the tropical marine boundary layer: description of the Fast LED-CE-DOAS instrument, Atmospheric Measurement Techniques, 7, 3579–3595, https://doi.org/10.5194/amt-7-3579-2014, 2014.

DiGangi, J. P., Henry, S. B., Kammrath, A., Boyle, E. S., Kaser, L., Schnitzhofer, R., Graus, M., Turnipseed, A., Park, J.-H., Weber, R. J., Hornbrook, R. S., Cantrell, C. A., Maudlin III, R. L., Kim, S., Nakashima, Y., Wolfe, G. M., Kajii, Y., Apel, E., Goldstein, A. H., Guenther, A., Karl, T., Hansel, A., and Keutsch, F. N.: Observations of glyoxal and formaldehyde as metrics for the anthropogenic impact on rural photochemistry, Atmospheric Chemistry and Physics, 12, 9529–9543, https://doi.org/10.5194/acp-12-9529-2012, 2012.

Donner, S., Lauster, B., Ziegler, S., Artaxo, P., Beirle, S., Gurk, C., Lamneck, M., and Wagner, T.: Investigating vertical gradients of trace gases and aerosol at the Amazon Tall Tower Observatory (ATTO) using MAX-DOAS measurements, in: EGU General Assembly Conference Abstracts, p. 7417, 2024.

Fayad, L., Coeur, C., Fagniez, T., Secordel, X., Houzel, N., Mouret, G., Ryan, R. G., Rhodes, S., Tully, M., and Schofield, R.: Surface ozone exceedances in Melbourne, Australia are shown to be under NOx control, as demonstrated using formaldehyde:NO2 and glyoxal:formaldehyde ratios, Science of The Total Environment, 749, 141 460, https://doi.org/10.1016/j.scitotenv.2020.141460, 2020.

Geng, C., Li, S., Yin, B., Gu, C., Liu, Y., Li, L., Li, K., Zhang, Y., Azzi, M., Li, H., Wang, X., Yang, W., and Bai, Z.: Atmospheric Carbonyl Compounds in the Central Taklimakan Desert in Summertime: Ambient Levels, Composition and Sources, Atmosphere, 13, 761, https://doi.org/10.3390/atmos13050761, 2022.

Grosjean, D., Grosjean, E., and Moreira, L. F. R.: Speciated Ambient Carbonyls in Rio de Janeiro, Brazil, Environmental Science & Technology, 36, 1389–1395, https://doi.org/10.1021/es0111232, 2002.

Guo, Y., Wang, S., Zhu, J., Zhang, R., Gao, S., Saiz-Lopez, A., and Zhou, B.: Atmospheric formaldehyde, glyoxal and their relations to ozone pollution under low- and high-NOx regimes in summertime Shanghai, China, Atmospheric Research, 258, 105 635, https://doi.org/10.1016/j.atmosres.2021.105635, 2021.

Henry, S. B., Kammrath, A., and Keutsch, F. N.: Quantification of gas-phase glyoxal and methylglyoxal via the Laser-Induced Phosphorescence of (methyl)GLyOxal Spectrometry (LIPGLOS) Method, Atmospheric Measurement Techniques, 5, 181–192, https://doi.org/10.5194/amt-5-181-2012, 2012.

Hettiyadura, A. P. S., Jayarathne, T., Baumann, K., Goldstein, A. H., de Gouw, J. A., Koss, A., Keutsch, F. N., Skog, K., and Stone, E. A.: Qualitative and quantitative analysis of atmospheric organosulfates in Centreville, Alabama, Atmospheric Chemistry and Physics, 17, 1343–1359, https://doi.org/10.5194/acp-17-1343-2017, 2017.

Hong, Q., Liu, C., Hu, Q., Zhang, Y., Xing, C., Jinping Ou, Tan, W., Liu, H., Huang, X., and Zhenfeng Wu: Vertical distribution and temporal evolution of formaldehyde and glyoxal derived from MAX-DOAS observations: The indicative role of VOC sources, Journal of Environmental Sciences-china, 122, 92–104, https://doi.org/10.1016/j.jes.2021.09.025, 2022.

Huang, H. B., Cheng, H. R., Hu, K., et al.: Characteristics and sources of dicarbonyl compounds during summer photochemical pollution episodes in Wuhan, China Environmental Science, 43, 5114–5122, 2023.

Ieda, T., Kitamor, Y., Mochida, M., Hirata, R., Hirano, T., Inukai, K., Fujinuma, Y., and Kawamura, K.: Diurnal variations and vertical gradients of biogenic volatile and semi-volatile organic compounds at the Tomakomai larch forest station in Japan, Tellus B: Chemical and Physical Meteorology, 58, https://b.tellusjournals.se/articles/10.1111/j.1600-0889.2006.00179.x, 2006.

Johnson, E. D.: Analysis of glyoxal concentrations among a deciduous forest canopy, Working Paper, University of Michigan Biological Station, http://deepblue.lib.umich.edu/handle/2027.42/62026, 2008.

Kaiser, J., Skog, K. M., Baumann, K., Bertman, S. B., Brown, S. B., Brune, W. H., Crounse, J. D., de Gouw, J. A., Edgerton, E. S., Feiner, P. A., Goldstein, A. H., Koss, A., Misztal, P. K., Nguyen, T. B., Olson, K. F., St. Clair, J. M., Teng, A. P., Toma, S., Wennberg, P. O., Wild, R. J., Zhang, L., and Keutsch, F. N.: Speciation of OH reactivity above the canopy of an isoprene-dominated forest, Atmospheric Chemistry and Physics, 16, 9349–9359, https://doi.org/10.5194/acp-16-9349-2016, 2016.

Kawamura, K., Okuzawa, K., Aggarwal, S. G., Irie, H., Kanaya, Y., and Wang, Z.: Determination of gaseous and particulate carbonyls (glycolaldehyde, hydroxyacetone, glyoxal, methylglyoxal, nonanal and decanal) in the atmosphere at Mt. Tai, Atmospheric Chemistry and Physics, 13, 5369–5380, https://doi.org/10.5194/acp-13-5369-2013, 2013.

Kluge, F., Hüneke, T., Lerot, C., Rosanka, S., Rotermund, M. K., Taraborrelli, D., Weyland, B., and Pfeilsticker, K.: Airborne glyoxal measurements in the marine and continental atmosphere: comparison with TROPOMI observations and EMAC simulations, Atmospheric Chemistry and Physics, 23, 1369–1401, https://doi.org/10.5194/acp-23-1369-2023, 2023.

Lawson, S. J., Selleck, P. W., Galbally, I. E., Keywood, M. D., Harvey, M. J., Lerot, C., Helmig, D., and Ristovski, Z.: Seasonal in situ observations of glyoxal and methylglyoxal over the temperate oceans of the Southern Hemisphere, Atmospheric Chemistry and Physics, 15, 223–240, https://doi.org/10.5194/acp-15-223-2015, 2015.

Li, Q., Gong, D., Wang, H., Wang, Y., Han, S., Wu, G., Deng, S., Yu, P., Wang, W., and Wang, B.: Rapid increase in atmospheric glyoxal and methylglyoxal concentrations in Lhasa, Tibetan Plateau: Potential sources and implications, Science of The Total Environment, 824, 153 782, https://doi.org/10.1016/j.scitotenv.2022.153782, 2022.

Liang, S., Qin, M., Xie, P., Duan, J., Fang, W., He, Y., Xu, J., Liu, J., Li, X., Tang, K., Meng, F., Ye, K., Liu, J., and Liu, W.: Development of an incoherent broadband cavity-enhanced absorption spectrometer for measurements of ambient glyoxal and NO_2 in a polluted urban environment, Earth System Science Data, 12, 2499–2512, https://doi.org/10.5194/amt-12-2499-2019, 2013.

Lin, H., Long, M. S., Sander, R., Sandu, A., Yantosca, R. M., Estrada, L. A., Shen, L., and Jacob, D. J.: An Adaptive Auto-Reduction Solver for Speeding Up Integration of Chemical Kinetics in Atmospheric Chemistry Models: Implementation and Evaluation in the Kinetic Pre-Processor (KPP) Version 3.0.0, Journal of Advances in Modeling Earth Systems, 15, e2022MS003 293, https://doi.org/10.1029/2022MS003293, 2023.

Liu, W., Zhang, J. J., Kwon, J., Weisel, C., Turpin, B., Zhang, L., Korn, L., Morandi, M., Stock, T., and Colome, S.: Concentrations and Source Characteristics of Airborne Carbonyl Compounds Measured Outside Urban Residences, Journal of the Air & Waste Management Association, 56, 1196–1204, https://doi.org/10.1080/10473289.2006.10464539, 2006.

MacDonald, S. M., Oetjen, H., Mahajan, A. S., Whalley, L. K., Edwards, P., Heard, D. E., Jones, C. E., and Plane, J. M. C.: DOAS measurements of formaldehyde and glyoxal above a south-east Asian tropical rainforest, Atmospheric Chemistry and Physics, 12, 5949–5962, https://doi.org/10.5194/acp-12-5949-2012, 2012.

Mitsuishi, K., Iwasaki, M., Takeuchi, M., Okochi, H., Kato, S., Ohira, S.-I., and Toda, K.: Diurnal Variations in Partitioning of Atmospheric Glyoxal and Methylglyoxal between Gas and Particles at the Ground Level and in the Free Troposphere, ACS Earth and Space Chemistry, 2, 915–924, https://doi.org/10.1021/acsearthspacechem.8b00037, 2018.

Possanzini, M., Tagliacozzo, G., and Cecinato, A.: Ambient Levels and Sources of Lower Carbonyls at Montelibretti, Rome (Italy), Water, Air, and Soil Pollution, 183, 447–454, https://doi.org/10.1007/s11270-007-9393-1, 2007.

Qi, W., Zhang, Y., Shen, M., Li, L., Dai, W., Chen, Y., Liu, Y., Guo, X., Cao, Y., Wang, X., Jiang, Y., and Li, J.: Comparison of gas–particle partitioning of glyoxal and methylglyoxal in the summertime atmosphere at the foot and top of Mount Hua, Molecules, 28, 5276, https://doi.org/10.3390/molecules28135276, 2023.

Sandu, A. and Sander, R.: Simulating chemical systems in Fortran90 and Matlab with the Kinetic PreProcessor KPP-2.1, Atmospheric Chemistry and Physics, 6, 187–195, https://doi.org/10.5194/acp-6-187-2006, 2006.

Seaman, V. Y., Charles, M. J., and Cahill, T. M.: A sensitive method for the quantification of acrolein and other volatile carbonyls in ambient air, Analytical Chemistry, 78, 2405–2412, https://doi.org/10.1021/ac051947s, 2006.

Sinreich, R., Coburn, S., Dix, B., and Volkamer, R.: Ship-based detection of glyoxal over the remote tropical Pacific Ocean, Atmospheric Chemistry and Physics, 10, 11 359–11 371, https://doi.org/10.5194/acp-10-11359-2010, 2010.

Spaulding, R. S., Schade, G. W., Goldstein, A. H., and Charles, M. J.: Characterization of secondary atmospheric photooxidation products: Evidence for biogenic and anthropogenic sources, Journal of Geophysical Research: Atmospheres, 108, https://doi.org/10.1029/2002JD002478, 2003.

Volkamer, R., San Martini, F., Molina, L. T., Salcedo, D., Jimenez, J. L., and Molina, M. J.: A missing sink for gas-phase glyoxal in Mexico City: Formation of secondary organic aerosol, Geophysical Research Letters, 34, https://doi.org/10.1029/2007GL030752, 2007.

Volkamer, R., Baidar, S., Campos, T. L., Coburn, S., DiGangi, J. P., Dix, B., Eloranta, E. W., Koenig, T. K., Morley, B., Ortega, I., Pierce, B. R., Reeves, M., Sinreich, R., Wang, S., Zondlo, M. A., and Romashkin, P. A.: Aircraft measurements of BrO, IO, glyoxal, NO_2, H_2O, O_2–O_2 and aerosol extinction profiles in the tropics: comparison with aircraft-/ship-based in situ and lidar measurements, Atmospheric Measurement Techniques, 8, 2121–2148, https://doi.org/10.5194/amt-8-2121-2015, 2015.

Walker, H., Stone, D., Ingham, T., Hackenberg, S., Cryer, D., Punjabi, S., Read, K., Lee, J., Whalley, L., Spracklen, D. V., Carpenter, L. J., Arnold, S. R., and Heard, D. E.: Observations and modelling of glyoxal in the tropical Atlantic marine boundary layer, Atmospheric Chemistry and Physics, 22, 5535–5557, https://doi.org/10.5194/acp-22-5535-2022, 2022.

Wang, Y., Dörner, S., Donner, S., Böhnke, S., De Smedt, I., Dickerson, R. R., Dong, Z., He, H., Li, Z., Li, Z., Li, D., Liu, D., Ren, X., Theys, N., Wang, Y., Wang, Y., Wang, Z., Xu, H., Xu, J., and Wagner, T.: Vertical profiles of NO_2, SO_2, HONO, HCHO, CHOCHO and aerosols derived from MAX-DOAS measurements at a rural site in the central western North China Plain and their relation to emission sources and effects of regional transport, Atmospheric Chemistry and Physics, 19, 5417–5449, https://doi.org/10.5194/acp-19-5417-2019, 2019.

Washenfelder, R. A., Young, C. J., Brown, S. S., Angevine, W. M., Atlas, E., Blake, D. R., Bon, D. M., Cubison, M. J., de Gouw, J. A., de Gouw, J. A., de Gouw, J. A., Dusanter, S., Flynn, J., Gilman, J. B., Graus, M., Griffith, S. M., Griffith, S. M., Grossberg, N., Hayes, P. L., Jimenez, J. L., Kuster, W. C., Lefer, B., Pollack, I. B., Ryerson, T. B., Ryerson, T. B., Stark, H., Stevens, P. S., and Trainer, M.: The glyoxal budget and its contribution to organic aerosol for Los Angeles, California, during CalNex 2010, Journal of Geophysical Research, 116, https://doi.org/10.1029/2011jd016314, 2011.

Wendisch, M., Pöschl, U., Andreae, M. O., Machado, L. A. T., Albrecht, R., Schlager, H., Rosenfeld, D., Martin, S. T., Abdelmonem, A., Afchine, A., Araùjo, A. C., Artaxo, P., Aufmhoff, H., Barbosa, H. M. J., Borrmann, S., Braga, R., Buchholz, B., Cecchini, M. A., Costa, A., Curtius, J., Dollner, M., Dorf, M., Dreiling, V., Ebert, V., Ehrlich, A., Ewald, F., Fisch, G., Fix, A., Frank, F., Fütterer, D., Heckl, C., Heidelberg, F., Hüneke, T., Jäkel, E., Järvinen, E., Jurkat, T., Kanter, S., Kästner, U., Kenntner, M., Kesselmeier, J., Klimach, T., Knecht, M., Kohl, R., Kölling, T., Krämer, M., Krüger, M., Krisna, T. C., Lavric, J. V., Longo, K., Mahnke, C., Manzi, A. O., Mayer, B., Mertes, S., Minikin, A., Molleker, S., Münch, S., Nillius, B., Pfeilsticker, K., Pöhlker, C., Roiger, A., Rose, D., Rosenow, D., Sauer, D., Schnaiter, M., Schneider, J., Schulz, C., de Souza, R. A. F., Spanu, A., Stock, P., Vila, D., Voigt, C., Walser, A., Walter, D., Weigel, R., Weinzierl, B., Werner, F., Yamasoe, M. A., Ziereis, H., Zinner, T., and Zöger, M.: ACRIDICON–CHUVA Campaign: Studying Tropical Deep Convective Clouds and Precipitation over Amazonia Using the New German Research Aircraft HALO, Bulletin of the American Meteorological Society, 97, 1885–1908, https://doi.org/10.1175/BAMS-D-14-00255.1, 2016.

Wolfe, G. M., Cantrell, C., Kim, S., Mauldin III, R. L., Karl, T., Harley, P., Turnipseed, A., Zheng, W., Flocke, F., Apel, E. C., Hornbrook, R. S., Hall, S. R., Ullmann, K., Henry, S. B., DiGangi, J. P., Boyle, E. S., Kaser, L., Schnitzhofer, R., Hansel, A., Graus, M., Nakashima, Y., Kajii, Y., Guenther, A., and Keutsch, F. N.: Missing peroxy radical sources within a summertime ponderosa pine forest, Atmospheric Chemistry and Physics, 14, 4715–4732, https://doi.org/10.5194/acp-14-4715-2014, 2014.

Wu, C., Wang, C., Wang, S., Wang, W., Yuan, B., Qi, J., Wang, B., Wang, H., Wang, C., Song, W., Wang, X., Hu, W., Lou, S., Ye, C., Peng, Y., Wang, Z., Huangfu, Y., Xie, Y., Zhu, M., Zheng, J., Wang, X., Jiang, B., Zhang, Z., and Shao, M.: Measurement report: Important contributions of oxygenated compounds to emissions and chemistry of volatile organic compounds in urban air, Atmospheric Chemistry and Physics, 20, 14 769–14 785, https://doi.org/10.5194/acp-20-14769-2020, 2020.

Xing, C., Liu, C., Hu, Q., Fu, Q., Lin, H., Wang, S., Su, W., Wang, W., Javed, Z., and Liu, J.: Identifying the wintertime sources of volatile organic compounds (VOCs) from MAX-DOAS measured formaldehyde and glyoxal in Chongqing, southwest China, Science of The Total Environment, 715, 136 258, https://doi.org/10.1016/j.scitotenv.2019.136258, 2020.

Xiong, E., Guo, H., Fu, T.-M., Lyu, X., Wang, Y., Zhou, B., Xia, M., Zou, Z., Yuan, Q., Yang, J., Shek, K. Y., Chen, J., Jiang, T., Tao, W., Zhang, A., Xiang, W., Lee, S., and Wang, T.: Complex impacts of oxygenated volatile organic compounds on radical photochemistry in the background air of Southern China, Submitted, 2025.

Xu, Y., Feng, X., Chen, Y., Zheng, P., Hui, L., Chen, Y., Yu, J. Z., and Wang, Z.: Development of an enhanced method for atmospheric carbonyls and characterizing their roles in photochemistry in subtropical Hong Kong, Science of The Total Environment, 896, 165 135, https://doi.org/10.1016/j.scitotenv.2023.165135, 2023.

Zhang, Y., Dai, W., Li, J., Ho, S. S. H., Li, L., Shen, M., Wang, Q., and Cao, J.: Comprehensive observations of carbonyls of Mt. Hua in Central China: Vertical distribution and effects on ozone formation, Science of The Total Environment, 907, 167 983, https://doi.org/10.1016/j.scitotenv.2023.167983, 2024.

Zhou, X. and Mopper, K.: Apparent partition coefficients of 15 carbonyl compounds between air and seawater and between air and freshwater; implications for air-sea exchange, Environmental Science & Technology, 24, 1864–1869, https://doi.org/10.1021/es00082a013, 1990a.

Zhou, X. and Mopper, K.: Measurement of sub-parts-per-billion levels of carbonyl compounds in marine air by a simple cartridge trapping procedure followed by liquid chromatography, Environmental Science & Technology, 24, 1482–1485, https://doi.org/10.1021/es00080a004, 1990b.

Zhu, B., Huang, X.-F., Xia, S.-Y., Lin, L.-L., Cheng, Y., and He, L.-Y.: Biomass-burning emissions could significantly enhance the atmospheric oxidizing capacity in continental air pollution, Environmental Pollution, 285, 117 523, https://doi.org/10.1016/j.envpol.2021.117523, 2021.

Zou, Z., Chen, Q., Xia, M., Yuan, Q., Chen, Y., Wang, Y., Xiong, E., Wang, Z., and Wang, T.: OH measurements in the coastal atmosphere of South China: possible missing OH sinks in aged air masses, Atmospheric Chemistry and Physics, 23, 7057–7074, https://doi.org/10.5194/acp-23-7057-2023, 2023.